Geophysical Research Letters

Key Points:
- Interannual variability of South Atlantic Ocean heat is determined by different mechanisms in high- and low-resolution simulations
- Signals enter from the south in the high-resolution and from the north in the low-resolution simulation
- Ekman heat transport contributes significantly in the low-resolution while geostrophic heat transport dominates in the high-resolution

Supporting Information:
- Supporting Information S1

Correspondence to:
A. Gronholz,
alexandra.gronholz@mpimet.mpg.de

Interannual Variability of the South Atlantic Ocean Heat Content in a High-Resolution Versus a Low-Resolution General Circulation Model

Alexandra Gronholz[1,2,3] , **Shenfu Dong[2]** , **Hosmay Lopez[2]**, **Sang-Ki Lee[2]** , **Gustavo Goni[2]** , and **Molly Baringer[2]**

[1]Cooperative Institute for Marine and Atmospheric Studies, University of Miami, Miami, FL, USA, [2]NOAA Atlantic Oceanographic and Meteorological Laboratory, Miami, FL, USA, [3]Max Planck Institute for Meteorology, Hamburg, Germany

Abstract High- and low-resolution coupled climate model simulations are analyzed to investigate the impact of model resolution on South Atlantic Ocean Heat Content (OHC) variability at interannual time scale and the associated physical mechanisms. In both models, ocean heat transport convergence is the main driver of OHC variability on interannual time scales. However, the origin of the meridional heat transport (MHT) convergence anomalies differs in the two models. In the high-resolution model, OHC variability is dominated by MHT from the south. This is in contrast to the low-resolution model, where OHC variability is largely controlled by MHT from the north. In the low-resolution simulation, both the Ekman and geostrophic transports contribute to the OHC variability, whereas in the high-resolution model, the geostrophic transport dominates. These differences highlight the importance of model resolution to appropriately represent ocean dynamics in the South Atlantic Ocean and associated impacts on regional and global climate.

Plain Language Summary In this study we analyze heat content changes of the upper South Atlantic Ocean and the impact of model resolution on these changes. Results from two numerical simulations are compared. One simulation with high-resolution allows smaller-scale processes directly, while the other simulation with low-resolution does not. In both simulations oceanic heat transport dominates the ocean heat content changes on interannual time scale, while atmospheric fluxes play a secondary role. The heat anomalies, however, originate from different regions in the two simulations. While the oceanic heat transport from the south dominates in the high-resolution simulation, oceanic heat transport from the north dominates in the low-resolution simulation. Furthermore, wind-induced surface heat transport plays a significant role in the low-resolution while the heat transport in the high-resolution simulation is dominated by changes in the ocean density field at depth. These results suggest fundamentally different driving mechanisms between the simulations and highlight the importance of model resolution to appropriately represent ocean dynamics in the South Atlantic Ocean and associated impacts on large-scale climate.

1. Introduction

The South Atlantic has a unique characteristic as it is the only ocean basin that transports heat equatorward, which results in an export of heat crossing the equator toward the Northern Hemisphere (e.g., Haarsma et al., 2009; Talley, 2003). This equatorward heat transport arises mainly from the Atlantic Meridional Overturning Circulation (AMOC) in contrast to other basins where the heat transport is dominated by gyre circulation and directed poleward. Earlier studies have suggested that changes in the transport and distribution of upper ocean heat across the South Atlantic could influence rainfall pattern over Africa and South America (e.g., Carton et al., 1996; Diaz et al., 1998; Moura & Shukla, 1982; Nobre & Shukla, 1996). More recently, Lopez, Dong, Lee, and Goni (2016) described how multidecadal variability of the Meridional Heat Transport (MHT) in the South Atlantic affects the global atmospheric circulation due to changes in the South Atlantic Ocean Heat Content (OHC). They concluded that the southern part of the AMOC is a potential predictor of global monsoon variability with a time lag of about one or two

decades. These studies highlight the importance of a detailed understanding of the South Atlantic OHC variability as well as the associated MHT and overturning.

In the conventional view, the AMOC is largely modulated by deep convection activity in the high-latitude sinking regions in the North Atlantic (e.g., Dickson & Brown, 1994; Dong & Sutton, 2005; Marshall & Schott, 1999; Msadek & Frankignoul, 2009). However, recent studies have suggested the possibility of the southern origin of AMOC variability and associated MHT anomalies, driven by changes in the Southern Hemisphere winds that impact, on the one hand, northward Ekman transport and upwelling (e.g., Gnanadesikan, 1999; Kuhlbrodt et al., 2007; McDermott, 1996; Oke & England, 2004; Speich et al., 2007; Toggweiler & Samuels, 1998), and on the other hand, signals entering from the Indian ocean via the Agulhas leakage (e.g., Biastoch et al., 2008; Donners & Drijfhout, 2004; Weijer et al., 1999, 2001). These mechanisms are highly impacted by ocean eddy processes and thus might be better represented in high-resolution simulations compared to low-resolution simulations. Specifically, the increased northward Ekman transport resulting from increased SH westerlies can be largely compensated by an accompanying increase in the southward eddy-induced transport, which reduces drastically the response of the AMOC to westerlies in eddy-resolving simulations (e.g., Hallberg & Gnanadesikan, 2006). In the second mechanism, Agulhas leakage processes may modify MHT on different time scales: density perturbations resulting in barotropic or baroclinic Kelvin waves could impact MHT on interannual to decadal scales (e.g., Biastoch et al., 2008; Weijer et al., 2002). On longer time scales, it is rather advective processes that modify AMOC (e.g., Biastoch et al., 2009; Weijer et al., 2002) which in turn is associated with the MHT. Intensity in wind stress curl over the Indian Ocean (e.g., Rouault et al., 2009) and a southward shift and strengthening of Southern Hemisphere westerlies (e.g., Beal et al., 2011; Biastoch et al., 2009; Durgadoo et al., 2013) can impact Agulhas leakage. These mechanisms have been intensely debated in terms of how the Agulhas leakage and eddy fluxes respond to the observed and projected changes in surface winds in the course of anthropogenic climate change. Those debates are fueled by the inability of current climate models in resolving mesoscale ocean eddies, which is a likely cause for large uncertainties in their results. Indeed, Volkov et al. (2008) showed that up to 42% of the total variance of the South Atlantic MHT is driven by eddy heat transport in an eddy-permitting resolution model. This is a considerably large amount while studies based on lower-resolution simulations define the eddy contribution as a minor contributor to the time dependency of the heat transport (e.g., Jayne & Marotzke, 2001).

Several key areas exist in the South Atlantic Ocean which potentially can drive OHC variability. These areas include the highly eddy-active Brazil-Malvinas confluence zone southwest of the study domain, and the southeastern boundary region affected by the Agulhas leakage. Another key area is where the South Equatorial Current bifurcates into the North Brazil Current and Brazil Current with vigorous atmosphere-ocean interactions (e.g., Rodrigues et al., 2007). Previous studies on those key regions are based on coarse resolution climate models (e.g., Haarsma et al., 2005; Wainer & Venegas, 2002), which do not explicitly represent mesoscale eddies in the ocean, or based on ocean-only models (e.g., Durgadoo et al., 2013; Schwarzkopf et al., 2019). Recent studies suggested that SST variability in the South Atlantic can also be remotely forced by changes in the tropical Pacific related to ENSO processes (e.g., Dong et al., 2020; Putrasahan et al., 2016) and Pacific multidecadal variability (Lopez, Dong, Lee, & Campos, 2016), which are due to natural interaction between the atmosphere and ocean. Therefore, high-resolution coupled models may provide more insightful understanding of the mechanisms for changes in the South Atlantic Ocean. Several recent studies have used fully coupled high-resolution models (Cheng et al., 2016; Putrasahan et al., 2015); however, their focus areas were mostly limited to the southeastern boundary region of Agulhas leakage; thus, these studies did not analyze all potential sources of OHC variability in terms of a heat budget analysis including advection and surface fluxes and did not perform a comparison between a low- and a high-resolution simulation, which is the main focus of the present study. The deficiencies of low-resolution simulations in capturing the eddy-driven features in the South Atlantic are clearly demonstrated in the comparison of the modeled sea surface height (SSH) fields with observations: Figure 1 illustrates the standard deviation of SSH from a high-resolution and a low-resolution model simulation in comparison with observations from AVISO satellite altimetry. The observed strong SSH variability due to eddy activity at both the western and eastern boundary regions are well reproduced in the high-resolution simulation (Figure 1b), but as expected, is not captured in the low-resolution simulation (Figure 1a). This indicates the importance of using a high-resolution ocean model to properly address South Atlantic Ocean dynamics. To our knowledge, this
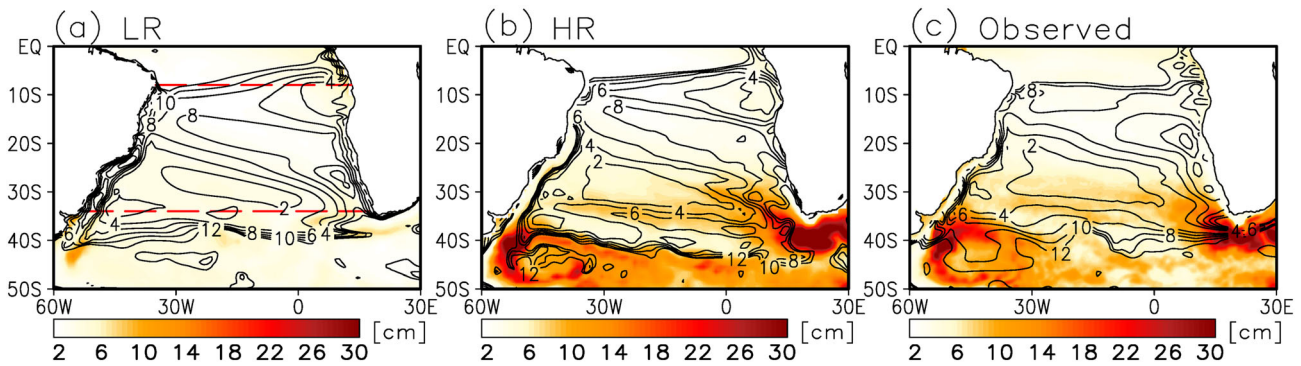
Figure 1. Standard deviation of sea surface height (SSH) and mean surface velocity contour lines (as $\sqrt{(u^2 + v^2)}$ in cm/s) from (a) low-resolution model simulation, (b) high-resolution model simulations, and (c) AVISO satellite altimeter (period 1993–2016) and NCEP GODAS reanalysis velocity data period is 1980–2020. Horizontal dashed red lines indicate the northern and southern boundaries for our study region. Aviso SSH has a 0.25° horizontal resolution, GODAS with 0.33° longitude and 1° latitude resolution, SSH from the low-resolution and high-resolution simulations are in 1° resolution. No temporal filtering was applied.

is the first study investigating interannual OHC variability and its origin in a global fully coupled high-resolution simulation, and providing an intercomparison analysis with an accompanying low-resolution simulation. Our analysis aims to quantify the impact of the northern versus southern origin of the OHC variability, and to determine the main drivers of the OHC variability in low- and high-resolution climate simulations. Given the physical link between the OHC variability and global monsoon rainfall variability identified in recent studies, the results from this study may have an important implication for the climate modeling community, particularly the need for a high-resolution for the simulations of interhemispheric Hadley circulation variability and its impact on global monsoon rainfall (e.g., Lopez, Dong, Lee, & Campos, 2016). This effect on larger-scale phenomena occurs via (upper) ocean-atmosphere interactions. Thus, this study focuses on the upper OHC of the upper 700 m.

2. Methods and Model Data

The two model simulations are based on the same version of the fully coupled Community Earth System Model (CESM, Gent et al., 2011; Hurrell et al., 2013) but with different horizontal grid resolutions. The coupled system consists of the Community Atmosphere Model version 5 (CAM5; Neale et al., 2010), the Parallel Ocean Program version 2 (POP2; Smith et al., 2010), the Community Land Model version 4 (Lawrence et al., 2011), and the Community Ice Code version 4 (Hunke & Lipscomb, 2008). The high-resolution simulation has a horizontal resolution of 0.1° for the ocean component and 62 z-levels. The atmospheric component has a 0.25° grid spacing and 30 vertical layers. The high-resolution simulation consists of 100 model years, while the first 14 years are removed and defined as spin-up years. Of the remaining 86 model years, only the last 46 years are analyzed in this study, to remove the nonlinear OHC increase during the first 40 years due to the model spin-up. The low-resolution simulation has a nominal 1° horizontal resolution and 60 levels in the ocean and an approximate 1° horizontal resolution in the atmosphere. The ocean model uses the Gent-McWilliams parameterization (Gent & Mcwilliams, 1990) to parameterize baroclinic instability and its effect on the ocean state, a submesoscale mixed layer eddy parameterization (Fox-Kemper et al., 2008) to approximate the results of high-resolution simulation, and an overflow parameterization (Danabasoglu et al., 2010) to represent overflows which are seen to be important for ocean circulation but which cannot directly be calculated in coarser resolution simulations due to their fine spatial scale. The simulation consists of 72 model years, exclusive of 94 spin-up years that are removed. Of these 72 years, our analysis begins with model year 20 to minimize a potential spin-up influence. Both simulations are run under "present-day" (year 2000) greenhouse gases conditions and thus variability in this study can be understood as intrinsic climate variability. More detailed information about the low- and high-resolution simulations can be found in Small et al. (2014).

The general ocean circulation is well captured in both simulations in terms of the basic pattern and the order of magnitude at the surface compared to the observed flow structure. However, differences can be observed in the southeastern South Atlantic, where the low-resolution simulation tends to create a rather zonal flow

to the west, which could impact the role of Agulhas leakage in the South Atlantic OHC changes. Furthermore, several other features in this region are not captured well in the low-resolution simulation, such as the northward intrusion and retroflection of the Malvinas Current.

We perform a heat budget analysis for the South Atlantic by defining the OHC as the upper 700 m heat content bounded between 34°S and 8°S. Over this depth range the spin-up time seems to be sufficient to allow for the OHC to reach a stable state, although it still experiences a slight decreasing trend after the spin-up period, which is removed by a least-square linear regression. The temporal changes in the OHC (i.e., heat storage rate) comprise of the sum of the MHT convergence (MHT_{con}, e.g., MHT at 34°S as MHT_{south} minus MHT at 8°S as MHT_{north}), vertical heat transport at 700 m depth (VHT700), and the net surface radiative and turbulent heat fluxes (Q_{net}). Using the monthly outputs of T, S, and the heat transport product (i.e., the model output product of temperature and velocity VT, including the VT_ISOP contribution to consider the parameterized transport based on eddy-induced velocities in the low-resolution simulation) from both simulations, OHC and MHT are calculated following methods described in Meyssignac et al. (2019) and Johns et al. (2011), respectively, as shown in the supporting information. Following Johns et al. (2011), the Ekman heat transport component is computed from model wind stress and the temperature averaged in the Ekman layer, consisting of the upper 50 m (e.g., Payne, 2003), by integrating across the basin. We note that the temperature, salinity, and the zonal wind stress are averaged meridionally over 3° for the high-resolution simulation to average out small-scale variabilities. Geostrophic heat transport is calculated as a residual between the total heat transport and the Ekman component. To further assess contributions of eddy-driven temperature and velocity anomalies and their correlation on the heat transport changes, we apply a Reynolds decomposition of MHT anomalies for the high-resolution simulation as described by Zhao et al. (2018) as shown in Text S1. For this, we define eddy impacts in the Agulhas region as variability on time scales up to 5 months (e.g., Cecilio et al., 2014), thus we calculate the temporal mean in Zhao et al. (2018) as the 5-month running-mean time series and the fluctuations as deviation from this mean.

To consider the nonzero net mass flux through each section due to integrating only over the upper 700 m instead of the entire water column, our heat transports should not be understood as "true heat transports" but as heat transports to a reference temperature of 0°C, as widely applied in literature (e.g., Hall & Bryden, 1982; Johns et al., 2011). As our analysis focuses on the interannual variability, all timeseries presented are smoothed by applying a 3-year running mean after removing seasonal cycle and a potential linear trend. The seasonal cycle is removed by subtracting the mean value for each month (January to December) of the entire time series from the actual month.

3. Results

Time series of OHC and contributions from surface air-sea heat fluxes, MHT convergence, and vertical heat transport at 700 m depth on interannual time scales are shown in Figure 2. In this section, we provide analyses as follows: we begin with analyzing the integrated time series and their impact on OHC variability, which is followed by a lead-lag correlation analysis of the nonintegrated heat budget terms. In this analysis, we start with the total heat convergence and then investigate in more detail the contributions from the northern and southern boundary. Finally, we give an overview of the contributions of Ekman and geostrophic components at both boundaries on the total heat transports.

Examination of the contributions from the integrated monthly data of surface heat fluxes and MHT convergence (Figures 2a and 2c) shows that on interannual to longer time scales, both the surface fluxes and oceanic processes are important for the OHC variability in the low-resolution simulation. However, in the high-resolution simulation, the OHC variability is dominated by the oceanic processes (i.e., MHT_{con} + VHT700). In the low-resolution simulation, both the integrated Q_{net} and MHT_{con} + VHT700 are significantly correlated with OHC with correlations of $r_{OHC\_Qnet} = 0.52 \pm 0.46$ and $r_{OHC\_adv} = 0.45 \pm 0.44$, respectively (confidence intervals here and hereafter were calculated using the 95% significance level; "adv" refers to the total of advective processes). The regression analysis gives the same conclusions with regression coefficients of $b_{OHC\_Qnet} = 0.56$ and $b_{OHC\_adv} = 0.43$, respectively. In the high-resolution simulation, the OHC variability is highly correlated with oceanic processes, with correlation of $r_{OHC\_adv} = 0.78 \pm 0.49$ and regression coefficient of $b_{OHC\_adv} = 0.72$, but no significant correlation with the integrated surface fluxes is found.
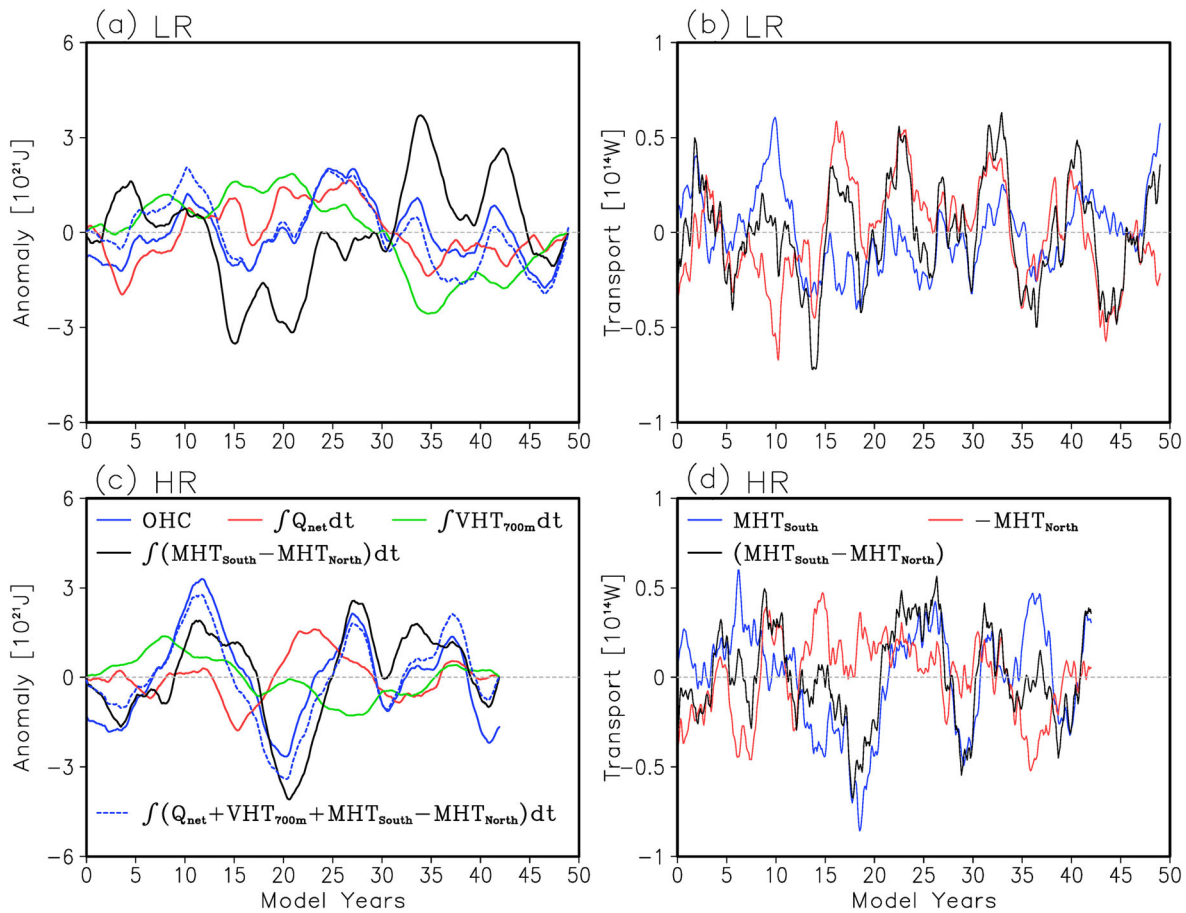
Figure 2. (left) Time series of OHC anomalies (blue, solid line), temporally integrated surface fluxes Q_{net} (red), MHT_{con} (black), vertical heat transport at 700 m (VHT700, green) and the sum of Q_{net}, MHT_{con}, and VHT700 (blue, dashed line); temporally integrated to correspond to OHC instead of its rate of change; (right) time series of the meridional heat transport (MHT) at the northern (MHT_{North}, 8°S, red) and southern (MHT_{South}, 34°S, blue) boundaries, and the corresponding oceanic heat convergence (MHT_{South} minus MHT_{North} as MHT_{con}, black); all as 3-year running mean; top panels are for low-resolution (a, b) and bottom panels for high-resolution (c, d) simulations.

For more details, we examine the lead-lag relationship of the nonintegrated budget terms with OHC variability. For the low-resolution simulation, both MHT convergence and vertical heat transport lead OHC, with MHT_{con} leading by 2 years with correlation of 0.45 ± 0.31, and the vertical heat transport at 700 m depth VHT700 leading by 1 year with negative correlation of -0.54 ± 0.36. Whereas the Qnet lags OHC by about 5 years with peak correlation of -0.34 ± 0.27, suggesting that ocean forces air-sea heat fluxes. MHT_{con} and VHT700 are strongly negatively correlated (-0.85 ± 0.3) and thus suggest VHT700 rather as a response to MHT_{con}. For the high-resolution simulation, the MHT convergence also leads OHC by 2 years ($r = 0.63 \pm 0.37$), but no lead-lag correlation was found between VHT700 and OHC. The Qnet also lags OHC but with a shorter lag of 1 year ($r = -0.41 \pm 0.37$). Again, MHT_{con} and VHT700 are negatively correlated (-0.54 ± 0.36) and thus suggest VHT700 rather as a response to MHT_{con}. These analyses support the dominating impact of oceanic heat convergence on OHC as surface fluxes are lagging and anticorrelated with OHC on interannual time scales. VHT700 can be excluded as potential driver of OHC variability, since both variables are not significantly or only negatively correlated in the high- and low-resolution simulations, respectively. The high correlation between the integrated Qnet and OHC in the low-resolution simulation discussed before is driven by processes on decadal time scales, as suggested by the significant positive correlation between Qnet and OHC when Qnet leads OHC by 15 years (Figure S1).

Figures 2b and 2d show that the total convergence (MHT_{South}-MHT_{North}) is dominated by the northern boundary in the low-resolution simulation, and by the southern boundary in the high-resolution simulation. In the low-resolution simulation, lead-lag correlations of the heat transport at the southern and northern

boundary with OHC variability show the largest negative correlations when MHT_{north} leads OHC by 2 years ($r_{MHTnorth\_LR} = -0.49 \pm 0.37$), and when MHT_{south} leads OHC by 6 years ($r_{MHTsouth\_LR} = -0.42 \pm 0.39$). The negative sign of the maximum correlation at the southern boundary confirms that the northern boundary dominates in the low-resolution simulation, as the correlation at the southern boundary would need to be positive to act as a driver for OHC. In the high-resolution simulation the situation is different. The heat transport at the southern boundary leads OHC by about 2 years with correlation of 0.46 ± 0.43. No significant lead-lag correlation was found between MHT_{north} and OHC. This confirms the dominating effect of the southern boundary in the high-resolution simulation and thus a notable difference between the simulations.

To estimate whether the high-resolution simulation is systematically overestimating MHT_{south} due to a higher SSH variability (Figure 1), we compared MHT_{south} over the entire water column in the high-resolution simulation (0.47PW $\pm$ 0.27PW) with heat transports estimated from observations (XBT; 0.49 ± 0.23PW, Dong et al., 2015) and from a model (0.60 ± 0.27PW, Baringer & Garzolli, 2007) at similar latitudes. Both mean and variability are comparable with previous estimates, suggesting that the model did not overestimate the MHT_{south}. For the upper 700 m the mean heat transports are about 0.64PW $\pm$ 0.27PW for MHT_{South_HR}, 1.00PW $\pm$ 0.26PW for MHT_{North_HR}, 0.64PW $\pm$ 0.24PW for MHT_{South_LR}, and 0.83PW $\pm$ 0.26PW for MHT_{North_LR}.

To further investigate the different processes leading to the differences in the OHC variability, we separate the MHT at the southern and northern boundary into two components: the wind-forced Ekman transport and density-driven geostrophic transport. Figure 3 shows the total MHT anomalies (black line) as well as contributions from the Ekman (red line) and the geostrophic (blue line) components. In the low-resolution simulation (Figures 3a and 3c), both the Ekman and geostrophic transports contribute significantly to the total MHT variations, with the geostrophic transport playing a slightly larger role. The correlation of Ekman transport with the total MHT is $r_{Ekman\_north\_LR} = 0.48 \pm 0.37$ at the northern boundary and $r_{Ekman\_south\_LR} = 0.44 \pm 0.37$ at the southern boundary. The geostrophic heat transport shows a high correlation with the total MHT, with a correlation of $r_{geo\_north\_LR} = 0.72 \pm 0.37$ at the northern boundary and $r_{geo\_south\_LR} = 0.63 \pm 0.37$ at the southern boundary. In contrast, in the high-resolution simulation the total MHT is largely dominated by the geostrophic transport (Figures 3b and 3d). No significant correlation is found between the Ekman component and the total MHT at both the northern and southern boundaries. The geostrophic component is highly correlated with the total MHT, with correlations of $r_{geo\_north\_HR} = 0.91 \pm 0.35$ at the northern boundary and $r_{geo\_south\_HR} = 0.88 \pm 0.41$ at the southern boundary. A Reynolds decomposition of MHT variability as explained in Zhao et al. (2018) shows no strong direct impact of eddy terms on the total MHT_{south} on interannual time scales. However, as the magnitude and structure of mean flow can be significantly affected by eddy-eddy interactions (e.g., Lee, 2001), indirect impacts of eddies may play an important role.

4. Discussion

Our analyses suggest that, on interannual time scale, in both simulations the MHT convergence dominates and leads OHC changes while surface fluxes play a minor role and lag OHC variability, while on interannual to longer time scales, both the surface fluxes and oceanic processes are important for the OHC variability in the low-resolution simulation. Similar findings regarding interannual variations of the upper OHC are shown by Dong and Kelly (2004) in the North Atlantic while these OHC variations in turn force air-sea fluxes. Piecuch and Ponte (2012) also highlighted the important role of ocean heat transport in OHC changes relative to the effect of surface fluxes. They showed that, while surface fluxes dominate heat storage within the near surface in the South Atlantic, heat transport convergence is the main driver of heat content in the upper ocean. This agrees with the results presented here from both simulations. More interestingly, we found a major contribution of MHT at the northern (southern) boundary on OHC variability in the low- (high-) resolution simulation, leading OHC variability by about 2 years.

The dominating effect of the northern boundary in the low-resolution might result from the larger variability in both the Ekman (standard deviation: $1.8e^{13}$ W) and particularly the geostrophic ($2.3e^{13}$ W) transports at that latitude compared to the transport variability (Ekman $1.7e^{13}$ W and geostrophic $1.8e^{13}$ W) at the
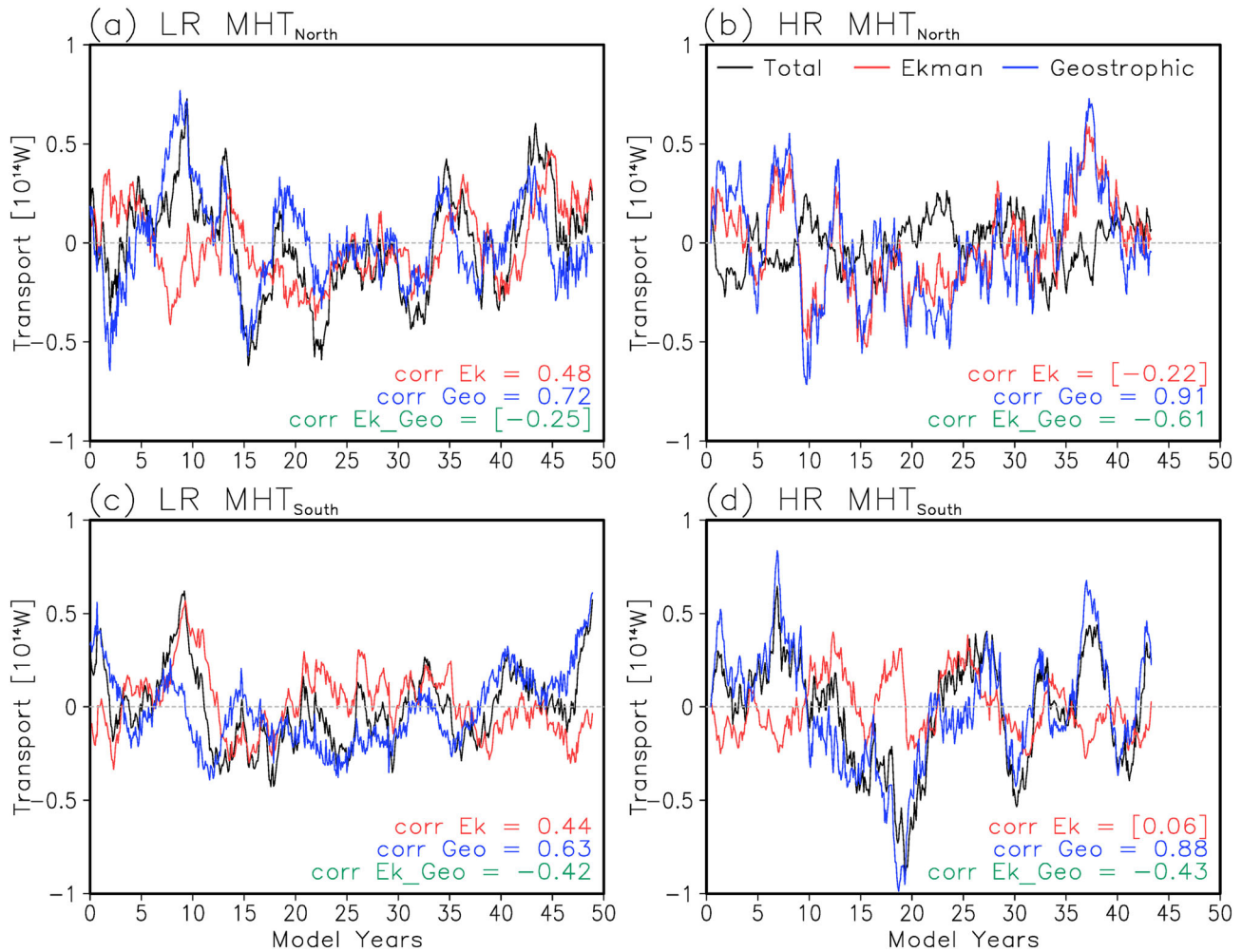
Figure 3. Interannual anomalies of MHT (black) and its Ekman (red) and geostrophic (blue) components at the northern (8°S) and southern (34°S) boundaries from the low-resolution (a, c) and high-resolution (b, d) simulations. Values indicate corresponding correlations, brackets for not significant correlations.

southern boundary, with no compensation between the Ekman and geostrophic heat transports (see values for corr$_{Ek\ Geo}$ in Figure 3). The dominating northern impact might be related to variabilities in the North Brazil Current, which are mainly wind-driven (Ruehs et al., 2015). It might also be a result of variabilities in the bifurcation latitude of the South Equatorial Current, which is strongly influenced by the local wind forcing and resulting Ekman transport and Ekman pumping (Rodrigues et al., 2007). The change of this latitude of bifurcation defines the interacting intensities of the Brazil Current (recirculating the heat in the South Atlantic) and the North Brazil Current (transporting it out).

The differences between the high- and the low-resolution simulations regarding the impact of the southern boundary might be partially a result of a different pathway of Agulhas leakage waters and partially of a more laminar behavior of the flow in the low-resolution simulation. The high-resolution allows the development of mesoscale features that are able to detach from the Agulhas Current and travel north-westward into the South Atlantic. In contrast, in the low-resolution simulation the incoming heat signals follow a rather zonal westward pathway and might enter the South Atlantic in a different way. This hypothesis is supported by the mean velocity field in the low-resolution simulation of the upper 700 m, which shows a rather continuing flow straight westward south of the South Atlantic domain as it is defined here. This suggests that the highly intermittent Agulhas leakage is not properly captured by the low-resolution simulation and the interocean exchange is through a rather laminar flow, which could reduce its impacts on OHC variability on interannual time scales. The findings of this work might be of particular importance for the adequate choice of model

resolution in studies that are strongly linked to OHC variability and its influence on climate and they are in agreement with a recent study by Roberts et al. (2020) who demonstrated that a high model resolution might be essential to represent MHT according to observations. It demonstrates the need for the application of high-resolution climate models when investigating processes such as rainfall pattern variability and monsoon modifications or predictions.

5. Summary and Conclusions

The South Atlantic has been shown to play an important role in the distribution of heat and fresh water globally, thus being capable of modulating large-scale climate pattern. In this study, we show that the OHC variability in the South Atlantic is driven by distinct processes in high- compared to low-resolution model simulations, leading to different interannual OHC variability. In both simulations, OHC changes on interannual time scales are controlled by the oceanic heat transport convergence/divergence, while surface air-sea heat fluxes play a minor role and lag OHC variability. However, marked differences can be observed between the low- and the high-resolution simulations. MHT at the northern boundary drives OHC variability in the low-resolution model, which is in contrast to the high-resolution model where OHC variability is predominately driven by MHT at the southern boundary. More importantly, differences are seen in the driving mechanism for the MHT variability in the two simulations. While the MHT variability in the low-resolution simulation is influenced by both the Ekman and geostrophic transport, in the high-resolution simulation the geostrophic transport controls the total MHT. These differences suggest the importance of model resolution in ocean simulations in order to investigate the oceanic heat budgets and to assess their potential larger-scale impacts on climate pattern or extreme weather events. These differences also highlight the need of long-term measurements in this region from arrays (Meinen et al., 2013; Speich et al., 2010) and from sustained ocean observations (Dong et al., 2015; Majumder et al., 2016) to better understand the oceanic dynamics and for model evaluation.

Although our study focuses on the impact of different resolutions of ocean model component, we acknowledge here that different atmospheric resolutions can also impact the results. Nevertheless, due to the feedbacks in a coupled system, the atmospheric state will never be exactly comparable when coupled to a low- and a high-resolution ocean component, even under the same atmospheric resolution. We also aim here to provide a direct applicable benefit to the geophysical community by comparing the two standard approaches of coupled climate modeling: the application of a coupled system with either low-resolution components as standard procedure, or with high-resolution components as new upcoming approach in times of increasing computational possibilities.

Data Availability Statement

The model outputs used in this study are available online (https://www.earthsystemgrid.org/dataset/ucar.cgd.asd.output.html). NCEP GODAS velocity data provided by Physical Sciences Division, Earth System Research Laboratory, NOAA, Boulder, Colorado, from their website (at https://psl.noaa.gov/). AVISO satellite data are available online (www.aviso.altimetry.fr) (global mesoscale eddy trajectory product).

References

Baringer, M. O., & Garzoli, S. L. (2007). Meridional heat transport determined with expendable bathythermographs—Part I: Error estimates from model and hydrographic data. *Deep Sea Research Part I: Oceanographic Research Papers*, *54*(8), 1390–1401.

Beal, L., de Ruijter, W. P., Biastoch, A., & Zahn, R. (2011). On the role of the Agulhas system in ocean circulation and climate. *Nature*, *472*(7344), 429–436. https://doi.org/10.1038/nature09983

Biastoch, A., Böning, C., & Lutjeharms, J. R. E. (2008). Agulhas leakage dynamics affects decadal variability in Atlantic overturning circulation. *Nature*, *456*(7221), 489–492. https://doi.org/10.1038/nature07426

Biastoch, A., Böning, C., Schwarzkopf, F., & Lutjeharms, J. R. E. (2009). Increase in Agulhas leakage due to poleward shift of southern hemisphere westerlies. *Nature*, *462*(7272), 495–498. https://doi.org/10.1038/nature08519

Carton, J. A., Cao, X., Giese, B. S., & Silva, A. M. D. (1996). Decadal and interannual SST variability in the tropical Atlantic Ocean. *Journal of Physical Oceanography*, *26*(7), 1165–1175.

Cecilio, C. M., Gherardi, D. F. M., Souza, R. B., & Correa-Ramirez, M. (2014). Spatio-Temporal variability of the eddy kinetic energy in the South Atlantic Ocean. *IEEE Geoscience and Remote Sensing Letters*, *11*(11), 2010–2014. https://doi.org/10.1109/lgrs.2014.2317414

Cheng, Y., Putrasahan, D., Beal, L., & Kirtman, B. (2016). Quantifying Agulhas leakage in a high-resolution climate model. *Journal of Climate*, *29*, 6881–6892.

Danabasoglu, G., Large, W. G., & Briegleb, B. P. (2010). Climate impacts of parameterized Nordic Sea overflows. *Journal of Geophysical Research*, *115*, C11005. https://doi.org/10.1029/2010JC006243

Diaz, A. F., Studzinski, C. D., & Mechoso, C. R. (1998). Relationships between precipitation anomalies in Uruguay and southern Brazil and sea surface temperature in the Pacific and Atlantic oceans. *Journal of Climate*, *11*(2), 251–271.

Dickson, R. R., & Brown, J. (1994). The production of North Atlantic Deep Water: Sources, rates, and pathways. *Journal of Geophysical Research*, *99*(C6), 12,319–12,341. https://doi.org/10.1029/94JC00530

Dong, B., & Sutton, R. T. (2005). Mechanism of interdecadal thermohaline circulation variability in a coupled ocean–atmosphere GCM. *Journal of Climate*, *18*, 1117–1135. https://doi.org/10.1175/JCLI3328.1

Dong, S., Goni, G., & Bringas, F. (2015). Temporal variability of the South Atlantic meridional overturning circulation between 20°S and 35°S. *Geophysical Research Letters*, *42*, 7655–7662. https://doi.org/10.1002/2015GL065603

Dong, S., & Kelly, K. A. (2004). Heat budget in the Gulf Stream region: The importance of heat storage and advection. *Journal of Physical Oceanography*, *34*(5), 1214–1231.

Dong, S., Lopez, H., Lee, S.-K., Meinen, C. S., Goni, G., & Baringer, M. (2020). What caused the large-scale heat deficit in the subtropical South Atlantic Ocean during 2009–2012? *Geophysical Research Letters*, *47*, e2020GL088206. https://doi.org/10.1029/2020GL088206

Donners, J., & Drijfhout, S. (2004). The Lagrangian view of South Atlantic interocean exchange in a global ocean model compared with inverse model results. *Journal of Physical Oceanography*, *34*(5), 1019–1035.

Durgadoo, J. V., Loveday, B. R., Reason, C. J. C., Penven, P., & Biastoch, A. (2013). Agulhas leakage predominantly responds to the southern hemisphere westerlies. *Journal of Physical Oceanography*, *43*(10), 2113–2131.

Fox-Kemper, B., Ferrari, R., & Hallberg, R. (2008). Parameterization of mixed layer eddies. Part I: Theory and diagnosis. *Journal of Physical Oceanography*, *38*, 1145–1165. https://doi.org/10.1175/2007JPO3792.1

Gent, P. R., Danabasoglu, G., Donner, L. J., Holland, M. M., Hunke, E. C., Jayne, S. R., et al. (2011). The Community Climate System Model version 4. *Journal of Climate*, *24*(19), 4973–4991.

Gent, P. R., & Mcwilliams, J. C. (1990). Isopycnal mixing in ocean circulation models. *Journal of Physical Oceanography*, *20*, 150–155.

Gnanadesikan, A. (1999). A simple predictive model for the structure of the oceanic pycnocline. *Science*, *283*(5410), 2077–2079. https://doi.org/10.1126/science.283.5410.2077

Haarsma, R. J., Campos, E. J., Hazeleger, W., Severijns, C., Piola, A. R., & Molteni, F. (2005). Dominant modes of variability in the South Atlantic: A study with a hierarchy of ocean–atmosphere models. *Journal of Climate*, *18*, 1719–1735. https://doi.org/10.1175/JCLI3370.1

Haarsma, R. J., Campos, E. J. D., Drijfhout, S., Hazeleger, W., & Severijns, C. (2009). Impacts of interruption of the Agulhas leakage on the tropical Atlantic in coupled ocean–atmosphere simulations. *Climate Dynamics*, *36*(5), 989–1003.

Hall, M. M., & Bryden, H. L. (1982). Direct estimates and mechanisms of ocean heat transport. *Deep Sea Research Part A*, *29*(3), 339–359.

Hallberg, R., & Gnanadesikan, A. (2006). The role of eddies in determining the structure and response of the wind-driven southern hemisphere overturning: Results from the modeling eddies in the Southern Ocean (meso) project. *Journal of Physical Oceanography*, *36*(12), 2232–2252.

Hunke, E. C., & Lipscomb, W. H. (2008). CICS: The Los Alamos sea ice model user's manual, version 4. Technical report, Los Alamos Natl. Lab., Los Alamos.

Hurrell, J. W., Holland, M. M., Gent, P. R., Ghan, S., Kay, J. E., Kushner, P. J., et al. (2013). The Community Earth System Model: A framework for collaborative research. *Bulletin of the American Meteorological Society*, *94*(9), 1339–1360. https://doi.org/10.1175/BAMS-D-12-00121.1

Jayne, S. R., & Marotzke, J. (2001). The dynamics of ocean heat transport variability. *Reviews of Geophysics*, *39*(3), 385–411.

Johns, W. E., Baringer, M. O., Beal, L. M., Cunningham, S. A., Kanzow, T., Bryden, H. L., et al. (2011). Continuous, array-based estimates of Atlantic Ocean heat transport at 26.5°N. *Journal of Climate*, *24*(10), 2429–2449. https://doi.org/10.1175/2010JCLI3997.1

Kuhlbrodt, T., Griesel, A., Montoya, M., Levermann, A., Hofmann, M., & Rahmstorf, S. (2007). On the driving processes of the Atlantic meridional overturning circulation. *Reviews of Geophysics*, *45*, RG2001. https://doi.org/10.1029/2004RG000166

Lawrence, D. M., Oleson, K. W., Flanner, M. G., Thornton, P. E., Swenson, S. C., Lawrence, P. J., et al. (2011). Parameterization improvements and functional and structural advances in version 4 of the Community Land Model. *Journal of Advances in Modeling Earth Systems*, *3*, M03001. https://doi.org/10.1029/2011MS000045

Lee, S. K. (2001). On the structure of supercritical western boundary currents. *Dynamics of Atmospheres and Oceans*, *33*(4), 303–319, ISSN 0377-0265. https://doi.org/10.1016/S0377-0265(01)00056-2

Lopez, H., Dong, S., Lee, S. K., & Campos, E. (2016). Remote influence of Interdecadal Pacific Oscillation on the South Atlantic meridional overturning circulation variability. *Geophysical Research Letters*, *43*, 8250–8258. https://doi.org/10.1002/2016GL069067

Lopez, H., Dong, S., Lee, S.-K., & Goni, G. (2016). Decadal modulations of interhemispheric global atmospheric circulations and monsoons by the South Atlantic meridional overturning circulation. *Journal of Climate*, *29*(5), 1831–1851.

Majumder, S., Schmidt, C., & Halliwell, G. (2016). An observations and model-based analysis of meridional transports in the South Atlantic. *Journal of Geophysical Research: Oceans*, *212*, 5622–5638. https://doi.org/10.1002/2016JC011693

Marshall, J., & Schott, F. (1999). Open-ocean convection: Observations, theory, and models. *Reviews of Geophysics*, *37*(1), 1–64. https://doi.org/10.1029/98RG02739

McDermott, D. A. (1996). The regulation of northern overturning by southern hemisphere winds. *Journal of Physical Oceanography*, *26*(7), 1234–1255.

Meinen, C. S., Speich, S., Perez, R. C., Dong, S., Piola, A. R., Garzoli, S. L., et al. (2013). Temporal variability of the meridional overturning circulation at 34.5°S: Results from two pilot boundary arrays in the South Atlantic. *Journal of Geophysical Research: Oceans*, *118*, 6461–6478. https://doi.org/10.1002/2013JC009228

Meyssignac, B., Boyer, T., Zhao, Z., Hakuba, M. Z., Landerer, F. W., Stammer, D., et al. (2019). Measuring global ocean heat content to estimate Earth's energy imbalance. *Frontiers in Marine Science*, *6*, 432. https://doi.org/10.3389/fmars.2019.00432

Moura, A., & Shukla, J. (1982). On the dynamics of droughts in northeast Brazil: Observations, theory and numerical experiments with a general circulation model. *Journal of the Atmospheric Sciences*, *38*(12), 2653–2675.

Msadek, R., & Frankignoul, C. (2009). Atlantic multidecadal oceanic variability and its influence on the atmosphere in a climate model. *Climate Dynamics*, *33*, 45–62. https://doi.org/10.1007/s00382-008-0452-0

Neale, R. B., Chen, C. C., Gettelman, A., Lauritzen, P. H., Park, S., Williamson, D. L., et al. (2010). Description of the NCAR Community Atmosphere Model (CAM 5.0). Technical report, Natl. Cent. Atmos. Res., Boulder, Colo.

Nobre, P., & Shukla, J. (1996). Variations of sea surface temperature, wind stress, and rainfall over the tropical Atlantic and South America. *Journal of Climate*, *9*(10), 2464–2479.

Oke, P. R., & England, M. H. (2004). Oceanic response to changes in the latitude of the southern hemisphere subpolar westerly winds. *Journal of Climate*, *17*(5), 1040–1054.

Payne, T. (2003). Dynamical paleoclimatology: Generalized theory of global climate change by Barry Saltzman, international geophysics series, vol. 80, academic press, San Diego, CA, 2001. 354. ISBN 0-12-617331-1 (hardback). *International Journal of Climatology*, *23*, 477–478. https://doi.org/10.1002/joc.879

Piecuch, C. G., & Ponte, R. M. (2012). Importance of circulation changes to Atlantic heat storage rates on seasonal and interannual time scales. *Journal of Climate*, *25*(1), 350–362.

Putrasahan, D., Kirtman, B. P., & Beal, L. M. (2016). Modulation of SST interannual variability in the Agulhas leakage region associated with ENSO. *Journal of Climate*, *29*, 7089–7102. https://doi.org/10.1175/JCLI-D-15-0172.1

Putrasahan, D. A., Beal, L. M., Kirtman, B. P., & Cheng, Y. (2015). A new Eulerian method to estimate "spicy" Agulhas leakage in climate models. *Geophysical Research Letters*, *42*, 4532–4539. https://doi.org/10.1002/2015GL064482

Roberts, M. J., Jackson, L. C., Roberts, C. D., Meccia, V., Docquier, D., Koenigk, T., et al. (2020). Sensitivity of the Atlantic Meridional Overturning Circulation to model resolution in CMIP6 HighResMIP simulations and implications for future changes. *Journal of Advances in Modeling Earth Systems*, *12*, e2019MS002014. https://doi.org/10.1029/2019MS002014

Rodrigues, R. R., Rothstein, L. M., & Wimbush, M. (2007). Seasonal variability of the south equatorial current bifurcation in the Atlantic Ocean: A numerical study. *Journal of Physical Oceanography*, *37*(1), 16–30.

Rouault, M., Penven, P., & Pohl, B. (2009). Warming in the Agulhas current system since the 1980's. *Geophysical Research Letters*, *36*, L12602. https://doi.org/10.1029/2009GL037987

Ruehs, S., Getzlaff, K., Durgadoo, J. V., Biastoch, A., & Boening, C. W. (2015). On the suitability of north Brazil current transport estimates for monitoring basin-scale AMOC changes. *Geophysical Research Letters*, *42*, 8072–8080. https://doi.org/10.1002/2015GL065695

Schwarzkopf, F. U., Biastoch, A., Böning, C. W., Chanut, J., Durgadoo, J. V., Getzlaff, K., et al. (2019). The INALT family—A set of high-resolution nests for the Agulhas current system within global NEMO ocean/sea-ice configurations. *Geoscientific Model Development*, *12*, 3329–3355. https://doi.org/10.5194/gmd-12-3329-2019

Small, R. J., Bacmeister, J., Bailey, D., Baker, A., Bishop, S., Bryan, F., et al. (2014). A new synoptic scale resolving global climate simulation using the Community Earth System Model. *Journal of Advances in Modeling Earth Systems*, *6*, 1065–1094. https://doi.org/10.1002/2014MS000363

Smith, R., Jones, P., Briegleb, B., Bryan, F., Danabasoglu, G., Dennis, J., et al. (2010). The Parallel Ocean Program (POP) reference manual. Technical report, Los Alamos Natl. Lab., Los Alamos.

Speich, S., Blanke, B., & Cai, W. (2007). Atlantic meridional overturning circulation and the southern hemisphere supergyre. *Geophysical Research Letters*, *34*, L23614. https://doi.org/10.1029/2007GL031583

Speich, S., Garzoli, S., Piola, A., & the SAMOC Community (2010). A monitoring system for the South Atlantic as a component of the MOC. In J. Hall, D. E. Harrison, D. Stammer (Eds.), *Proceedings of OceanObs'09: Sustained Ocean Observations and Information for Society (Annex), Venice, Italy, 21–25 September 2009*. ESA Publication WPP-306.

Talley, L. D. (2003). Shallow, intermediate, and deep overturning components of the global heat budget. *Journal of Physical Oceanography*, *33*(3), 530–560.

Toggweiler, J. R., & Samuels, B. (1998). On the oceans large-scale circulation near the limit of no vertical mixing. *Journal of Physical Oceanography*, *28*(9), 1832–1852.

Volkov, D. L., Lee, T., & Fu, L. (2008). Eddy-induced meridional heat transport in the ocean. *Geophysical Research Letters*, *35*, L20601. https://doi.org/10.1029/2008GL035490

Wainer, I., & Venegas, S. (2002). South Atlantic variability in the climate system model. *Journal of Climate*, *15*, 1408–1420.

Weijer, W., de Ruijter, W. P. M., & Dijkstra, H. A. (2001). Stability of the Atlantic Overturning Circulation: Competition between Bering Strait freshwater flux and Agulhas heat and salt sources. *Journal of Physical Oceanography*, *31*, 2385–2402.

Weijer, W., de Ruijter, W. P. M., Dijkstra, H. A., & van Leeuwen, P. J. (1999). Impact of interbasin exchange on the Atlantic overturning circulation. *Journal of Physical Oceanography*, *29*(9), 2266–2284.

Weijer, W., de Ruijter, W. P. M., Sterl, A., & Drijfhout, S. S. (2002). Response of the Atlantic overturning circulation to South Atlantic sources of buoyancy. *Global and Planetary Change*, *34*, 293–311.

Zhao, J., Bower, A., Yang, J., Lin, X., & Holliday, N. P. (2018). Meridional heat transport variability induced by mesoscale processes in the subpolar North Atlantic. *Nature Communications*, *9*(1), 1124. https://doi.org/10.1038/s41467-018-03134-x